International Orthopaedics (SICOT) (2011) 35:1229–1236
DOI 10.1007/s00264-010-1146-x

ORIGINAL PAPER

Custom-made composite scaffolds for segmental defect repair in long bones

Johannes C. Reichert · Martin E. Wullschleger · Amaia Cipitria · Jasmin Lienau · Tan K. Cheng · Michael A. Schütz · Georg N. Duda · Ulrich Nöth · Jochen Eulert · Dietmar W. Hutmacher

Received: 27 August 2010 / Revised: 18 October 2010 / Accepted: 18 October 2010 / Published online: 7 December 2010
© Springer-Verlag 2010

Abstract Current approaches for segmental bone defect reconstruction are restricted to autografts and allografts which possess osteoconductive, osteoinductive and osteogenic properties, but face significant disadvantages. The objective of this study was to compare the regenerative potential of scaffolds with different material composition but similar mechanical properties to autologous bone graft from the iliac crest in an ovine segmental defect model. After 12 weeks, in vivo specimens were analysed by X-ray imaging, torsion testing, micro-computed tomography and histology to assess amount, strength and structure of the newly formed bone. The highest amounts of bone neoformation with highest torsional moment values were observed in the autograft group and the lowest in the medical grade polycaprolactone and tricalcium phosphate composite group. The study results suggest that scaffolds based on aliphatic polyesters and ceramics, which are considered biologically inactive materials, induce only limited new bone formation but could be an equivalent alternative to autologous bone when combined with a biologically active stimulus such as bone morphogenetic proteins.

J. C. Reichert · M. E. Wullschleger · A. Cipitria · M. A. Schütz · D. W. Hutmacher (✉)
Institute of Health and Biomedical Innovation,
Queensland University of Technology,
Brisbane, Queensland, Australia
e-mail: dietmar.hutmacher@qut.edu.au

A. Cipitria · J. Lienau · G. N. Duda
Julius Wolff Institut & Center for Musculoskeletal Surgery,
Berlin-Brandenburg Center for Regenerative Therapy,
Charité - Universitätsmedizin Berlin,
Humboldt Universität und Freie Universität,
Berlin, Germany

T. K. Cheng
Temasek Engineering School, Temasek Polytechnic,
Tampines, Singapore

J. C. Reichert · U. Nöth · J. Eulert
Orthopaedic Center for Musculoskeletal Research,
Department of Orthopaedic Surgery, König-Ludwig-Haus,
Julius Maximilians University,
Würzburg, Germany

Introduction

The vast majority of fractures and bone defects heal spontaneously. The bone healing process is generally stimulated and directed by well-balanced biological and microenvironmental determinants. Nowadays, improved surgical techniques, implant designs and perioperative management strategies aim to account for these factors and have procured better treatment outcomes of complex fractures and other skeletal defects [1–3]. However, an imbalance of bone regeneration enhancing factors as found in compromised wound/soft tissue environments or biomechanical instability can result in large defects with limited intrinsic regeneration potential [4]. In humans, the tibial diaphysis represents the most common anatomical site for segmental bone defects to occur. This is related to the minimal muscle and soft tissue coverage on its anteromedial surface which both increases the risk of bone loss and complicates treatment [5]. Segmental defects still represent a considerable surgical, socioeconomic and research challenge, and greatly influence patients' quality of life [5, 6]. Commonly, such defects are treated by transplantation of bone autografts to augment and accelerate bone regeneration [7, 8]. The application of autografts, however, is associated with prolonged anaesthetic periods, limited availability, donor site morbidity (persistent pain and

haemorrhage), risk of infection and predisposition to failure [9, 10]. To avoid the limitations associated with the current standard treatment modalities, recent research has focused on scaffold-based bone engineering. In tissue engineering, applied scaffolds initially must provide sufficient mechanical strength and stiffness to substitute for the lost mechanical function in diseased or damaged tissues. Yet, scaffolds may not necessarily be required to provide complete mechanical equivalence to healthy tissue, but the stiffness and strength should be sufficient to provide structural support and allow transmission of regeneration enhancing forces to the host tissue site. Cell turnover and tissue remodelling are important to achieve stable biomechanical conditions and vascularisation at the host site. Hence, the three-dimensional (3-D) scaffold/tissue construction should maintain sufficient structural integrity during the in vitro and/or in vivo growth and remodelling process. The effective scaffold can be altered by selecting base materials of different moduli and/or varying scaffold porosity and pore architecture.

Bioresorbable aliphatic polyesters, such as polyglycolide, polylactide, polycaprolactone (PCL) and their copolymers, are suitable materials for the design and fabrication of biocompatible scaffolds due to only minimal inflammatory and immunological responses evoked. This is reflected in their track record for regulatory approval and available devices for clinical applications [11, 12]. These materials offer favourable surface chemistries for cell attachment, proliferation and differentiation, while degradation by-products are nontoxic and metabolised/eliminated via natural pathways. Furthermore, these thermoplastic polymers can easily be processed into 3-D scaffolds with the desired geometry and controlled porosity and interconnectivity applying modern computer-based solid free-form fabrication methods [13]. These methods allow the design of scaffolds with biomechanical properties within the lower range of cancellous bone.

In this study, it was postulated that custom-designed cylindrical scaffolds that display similar mechanical properties to cancellous bone might be suitable to augment segmental bone defects of the tibia.

Materials and methods

Scaffold fabrication and preparation

Scaffolds with two different material compositions (Fig. 1) measuring 18 mm in diameter and 20 mm in height were fabricated as reported elsewhere [14]. Briefly, the structural parameters of the scaffolds were tailored by computer-aided design and included 100% pore interconnectivity within a pore size of 350–500 μm size and a 0/90° lay-down pattern (Fig. 1). This architectural layout is particularly suitable for load-bearing tissue engineering applications since the fully interconnected network of scaffold fibres can withstand physiological and mechanical stress in a manner similar to cancellous bone graft for up to three months [15, 16]. Moreover, the architectural pattern allows retention of coagulating blood during the early phase of healing, and bone ingrowth at later stages. Prior to surgery, all scaffolds were treated with 1 M NaOH for six hours and washed five times with phosphate-buffered saline (PBS). Scaffold sterilisation was achieved by incubation in 70% ethanol for five minutes and UV irradiation for 30 minutes. For technical reasons, the medical grade polycaprolactone-tricalcium phosphate (mPCL-TCP) scaffolds were produced as cylinders. Prior to scaffold sterilisation, a biopsy punch (diameter six mm) was used to produce an inner duct to leave a scaffold comparable to the poly(L-lactide-co-D,L-lactide) (PLDLLA)-TCP-PCL scaffolds regarding shape and structure.

Biomechanical testing of scaffolds

Compression tests were performed on an Instron 5848 testing system (Instron, Melbourne, Australia) with a 500 N load cell (n=6). The specimens were compressed at a rate of 1 mm/min up to a strain level of approximately 5%. During the testing period, samples were kept in PBS under ambient conditions. The compression modulus was calculated and the compressive stiffness was determined from the stress-strain curve as the slope of the initial linear portion of the curve.

Segmental defect model

Twelve merino sheep (weight 45±2 kg, age seven years) were operated upon as approved by the University Animal Ethics Committee of the Queensland University of Technology, Brisbane, Australia (Ethics No.: 0700000915). All animals were in good health but of small stature (related to the geographic and climatic conditions in central Queensland, Australia). Animals were placed in right lateral recumbency. The right hindlimb was shaved and disinfected thoroughly. Under general anaesthesia, the tibia was exposed medially by a longitudinal 10-cm incision. A nine-hole, 4.5-mm narrow, limited contact locking compression plate (LC-LCP, Synthes) was applied to the anteromedial tibia. The implant, a modern internal fixation system, was chosen since it had previously been used with success to stabilise an experimental fracture in sheep femora (Wullschleger et al., unpublished data). The osteotomy lines were marked with a rasp, the plate was removed, the soft tissue in the designated defect area detached from the bone and parallel osteotomies perpendicular to the bone's longitudinal axis were performed with an oscillating saw (Stryker, Brisbane, Australia) under constant

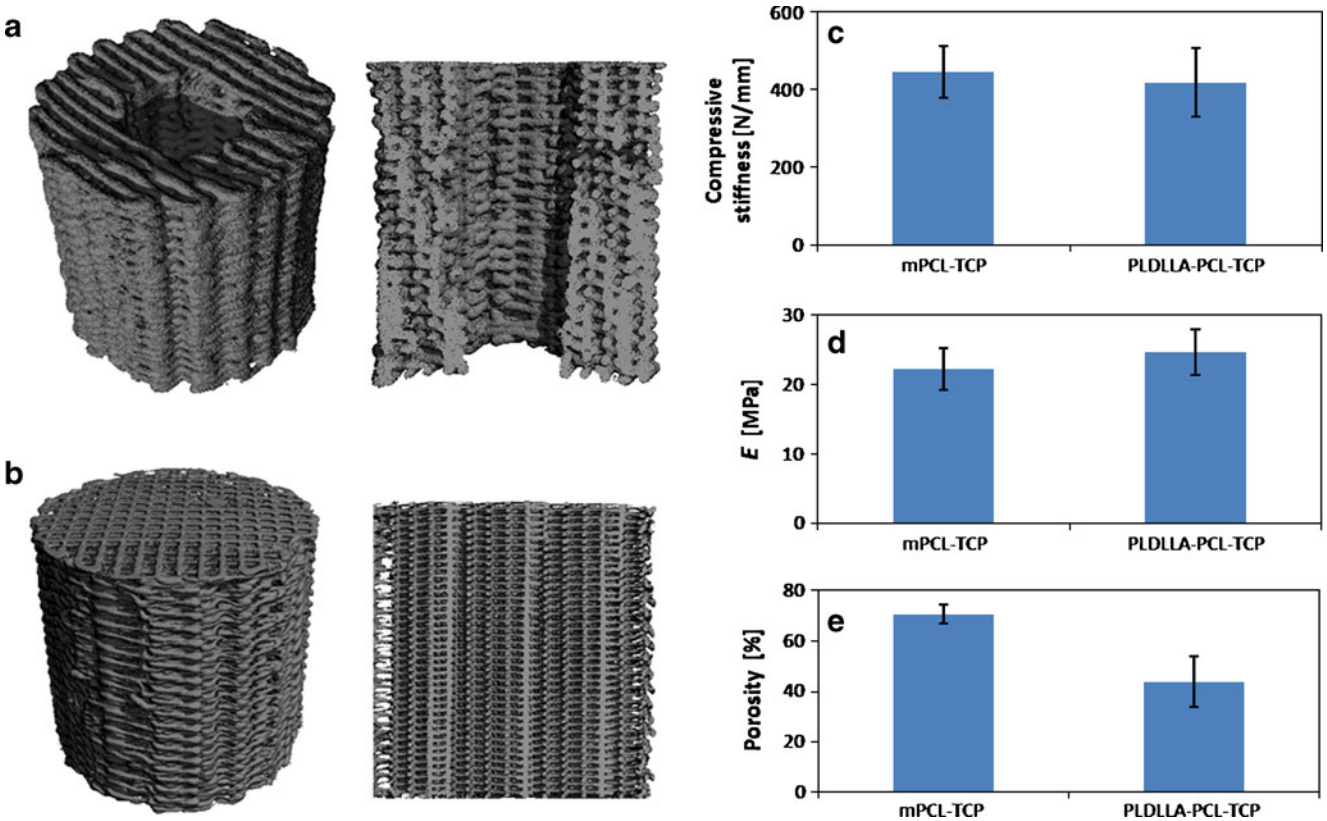

Fig. 1 MicroCT 3-D reconstructions of a PDLLA-TCP-PCL (**a**) and mPCL-TCP scaffold (**b**) (height 20 mm, diameter 18 mm). Compressive stiffness values averaged 446 N/mm (SD=66.3) for mPCL-TCP and 418 N/mm for PLDLLA-TCP-PCL (SD=88.1) scaffolds (**c**), the elastic modulus 22.17 MPa (SD 3.0) and 24.70 MPa (SD=3.3) (**d**), respectively. Scaffold porosity was determined to be 70.55% for mPCL-TCP (SD=3.78) scaffolds and 43.76% for PLDLLA-TCP-PCL (SD=10.02) scaffolds (**e**) as determined by microCT analysis. *Error bars* represent standard deviations, $n=6$

irrigation. Care was taken to completely remove the periosteum within the defect area. The bone fragments were realigned and fixed applying the LC-LCP with three bicortical screws proximally and three screws distally to leave a defect gap of exactly two cm size. Defects were left untreated, filled with autologous cancellous bone graft from the iliac crest or mPCL-TCP or PLDLLA-TCP-PCL scaffolds (Fig. 2). The wound was closed in layers, sprayed with OPSITE (Smith & Nephew, Mt. Waverley, Australia), covered with pads and bandaged with hard plaster (Vet-lite, Runlite SA, Micheroux, Belgium). The animals were held in a suspension trolley for 24 hours to allow recovery from anaesthesia prior to release into a paddock. The animals were allowed unrestricted weight-bearing. After 12 weeks, the animals were euthanised by intravenous injection of 60 mg/kg pentobarbital sodium (Lethabarb, Virbac, Australia).

Radiographic analysis

Immediately after surgery, after six and 12 weeks, conventional X-ray analysis (Phillips BV26) in two standard planes (anterior-posterior and medial-lateral) was performed to assess bone formation.

Biomechanical testing

Both ends of the tibiae were embedded in 80 ml Paladur (Heraeus Kulzer GmbH, Wehrheim, Germany) and mounted in an Instron 8874 biaxial testing machine (Instron, Melbourne, Australia). Care was taken to prevent samples from drying out. A torsion test was conducted at an angular velocity of 0.5°/s and a compressive load of 0.05 kN until the fracture point was reached (right tibiae counterclockwise, left tibiae clockwise). The contralateral tibia was used as a paired reference. The torsional moment (TM) and torsional stiffness (TS) were calculated from the slope of the torque-angular displacement curves and normalised against the values of the intact contralateral tibiae.

MicroCT analysis

For microCT analysis (μCT 40, Scanco, Brüttisellen, Switzerland), samples were scanned with a voxel size of

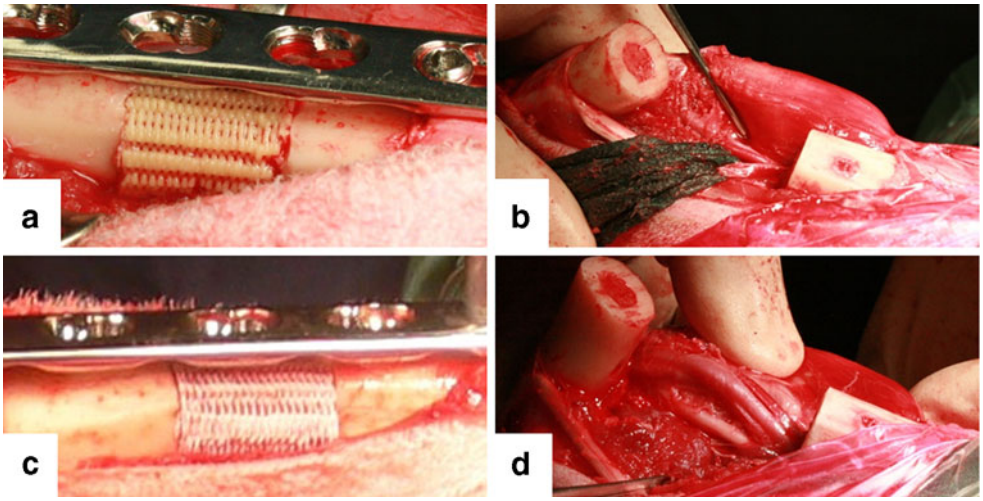

Fig. 2 Tibial segmental bone defect of 2 cm length stabilised with a limited contact locking compression plate (LC-LCP, Synthes) and filled with a PDLLA-TCP-PCL (**a**) and mPCL-TCP scaffold (**c**). Prior to scaffold insertion, the periosteum (**b**), which is in close proximity to the neurovascular bundle, was entirely removed within the defect area (**d**)

16 µm. The X-ray tube was operated at 55 kV and 145 µA. The image matrix size was 1,024×1,024 pixels. Samples were evaluated at a threshold of 220 HU, a filter width of 0.8 and filter support of 1.0. Bone volume within the defect, bone mineral density as well as trabecular number were quantified using software supplied by Scanco.

Histology

Specimens were fixed in 10% neutral buffered formalin and the mid-defect regions were sectioned in the transverse and sagittal planes. Callus tissue composition was evaluated on 6-µm-thick methyl methacrylate (Technovit 9100 NEU, Heraeus Kulzer, Wehrheim, Germany) embedded sections, stained with safranin orange/von Kossa (mineralised tissue black) and Movat's pentachrome [17] to demonstrate bone (yellow), cartilage (deep green) and fibrous tissue (light green-blue).

Statistical analysis

Statistical analysis was carried out using a two-tailed Mann-Whitney U test (SPSS 16.0), and p values <0.05 were considered significant. Correlation coefficients were calculated using the respective function in Microsoft Excel 2008 version 12.2.0.

Results

Scaffold characterisation

To achieve scaffolds of similar mechanical properties, melt extrusion/fused deposition modelling (FDM) parameters for the PLDLLA-TCP-PCL blend had to be adjusted to include filaments of larger diameter, which consecutively resulted in smaller pore size (Fig. 1). Scaffold porosity was determined to be 70.55% for mPCL-TCP (SD=3.78) scaffolds and 43.76% for PLDLLA-TCP-PCL (SD=10.02) scaffolds as determined by microCT analysis. Compressive stiffness values averaged 446 N/mm (SD=66.3) for mPCL-TCP and 418 N/mm for PLDLLA-TCP-PCL (SD=88.1) scaffolds. The elastic modulus calculated for mPCL-TCP scaffolds was 22.17 MPa (SD=3.0) and 24.70 MPa (SD=3.3) for scaffolds consisting of PLDLLA-TCP-PCL (Fig. 1).

In vivo performance of mPCL-TCP and PLDLLA-TCP-PCL scaffolds

Conventional X-ray analysis in two planes after 12 weeks showed a subcritical nature of the defect as defect bridging was observed in all animals of the empty control group. It was also found that minor plate bending (10–15°) had occurred in four animals. These animals were either treated with autologous bone graft (ABG) (two) or were left untreated (two). No screw loosening, implant breakage or tibial valgus deformity was observed. Only minor external callus and bone formation was observed in the scaffold groups. Callus was found to be located mainly posterolaterally. In all defects reconstructed with ABG, however, full defect bridging had occurred (Fig. 3). During dissection of the amputated limbs no macroscopic signs of inflammation/foreign body response to the implanted scaffolds were observed.

Von Kossa/van Gieson staining on histological polymethyl methacrylate (PMMA) sections (Fig. 4) revealed good scaffold integration with the host bone while the structure of the transplanted scaffold was well preserved. No signs of scaffold resorption were evident. The highest amounts of mineralised tissue (black) appeared in the ABG group. Both in the ABG and empty control groups more extensive new periosteal bone formation was observed on the posterolateral side (Fig. 4a, b and e, f) only a little

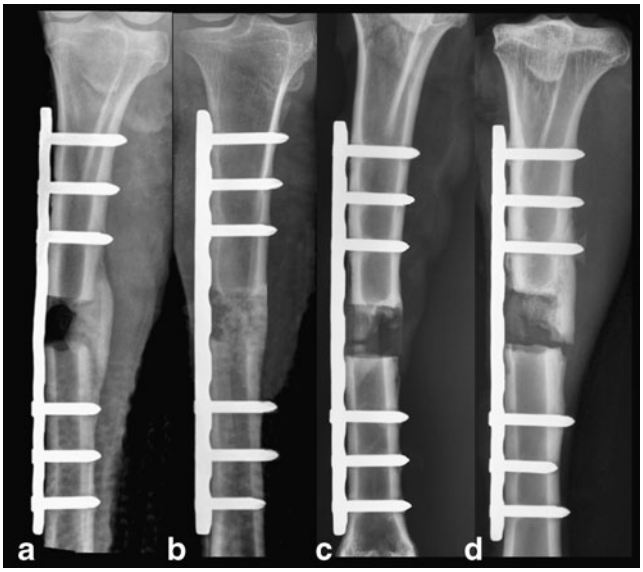

Fig. 3 X-ray images in the anterior-posterior plane of 2-cm tibial segmental bone defects left untreated (**a**), reconstructed with ABG (**b**), a mPCL-TCP scaffold (**c**) or a PDLLA-TCP-PCL scaffold (**d**) 12 weeks after surgery. The images show the subcritical nature of the defect as bridging was observed in the empty control defect. Homogeneous bone formation and bridging throughout the defect was observed when treated with ABG. Less bone and discontinuous bridging occurred in the scaffold groups

medially close to the plate. In contrast, bone formation evident in the scaffold groups appeared to be endosteal (Fig. 4c, d). No increased levels of inflammatory cells were found in sections of scaffold-treated defects. In any case, bone formation seemed to occur through chondral stages (endochondral bone formation) (Fig. 4i) leading to subsequent osteoid formation (Fig. 4j) as assessed in Movat's pentachrome stainings. In the ABG reconstructed defects first signs of bone remodelling processes were observed represented by osteoclastic and giant cells within the defect site (Fig. 4k).

Biomechanical testing (Fig. 5a) revealed higher TM values for the ABG (median=18.67 %) and PLDLLA-TCP-PCL (14.46 %) groups when compared to the mPCL-TCP group (4.96 %) or empty control (11.19 %). MicroCT evaluation correlated well with the biomechanical testing data (correlation coefficient 0.902) and confirmed the histology results showing the highest amount of bone formation in defects reconstructed with ABG (47.64%). Lower amounts of bone were recorded for the empty defects (31.7%) and the PLDLLA-TCP-PCL-augmented defects (30.43%), while a relative bone volume of only 11.96% was found for the mPCL-TCP-treated animals. Similar trends were reflected in the quantitative analysis of trabecular number (1/mm) and connectivity density (1/mm^3), which again showed highest values for the ABG (2.28/mm; 9.91/mm^3) followed by PLDLLA-TCP-PCL (1.14/mm; 7.71/mm^3), empty control defect (0.73/mm; 5.47/mm^3) and mPCL-TCP-filled defects (0.39/mm; 2.22/mm^3). No differences in mineral density of the newly formed bone were found between the different groups (Fig. 5).

Discussion

Well-established clinical therapeutic approaches for long bone reconstruction are restricted to bone transport or autograft and allograft transplantation. Bone grafts possess osteoconductive and osteoinductive properties, are however limited in access and availability and associated with donor site morbidity, haemorrhage, risk of infection, insufficient transplant integration, graft devitalisation and subsequent resorption resulting in decreased mechanical stability [9, 10]. As a result, recent research has focused on the development of alternative therapeutic concepts. The field of tissue engineering has emerged as an important approach to bone regeneration. Critical variables in scaffold design and function include the bulk material or components the bulk material consists of, 3-D architecture, surface chemistry, mechanical properties, the initial environmental conditions in the area around the scaffold and the environment surrounding the scaffold later on in the regenerative process, which is often determined by degradation characteristics. Scaffolds for the treatment of critical-sized segmental defects of the tibia and femur will have to meet certain minimum requirements from a biochemical, chemical and physical perspective. Scaffolds are not required to provide complete mechanical equivalence to the long bones, but stiffness and strength should be sufficient to at least support and transmit a fraction of the forces to the host tissue site, similar to autografts harvested from the iliac crest.

Long bone engineering approaches require scaffolds that balance temporary mechanical function with morphological properties (pore architecture, size and interconnectivity) to aid biological delivery and tissue regeneration. Such complex scaffold architectures can be achieved using layer-by-layer manufacturing processes (solid free-form fabrication) such as FDM [18].

Aliphatic polyesters such as PLLA/PDLA, PLLLA/PGA, PCL and others have demonstrated excellent safety profiles in multiple in vitro, animal and clinical studies and have received approval for clinical applications mainly in the oral and maxillofacial region [19–21]. Polymer/calcium phosphate composites such as mPCL-TCP or PDLLA-TCP-PCL confer favourable mechanical and biochemical properties, including strength via the ceramic phase and toughness and plasticity via the polymer phase. They possess more favourable degradation and resorption kinetics, and

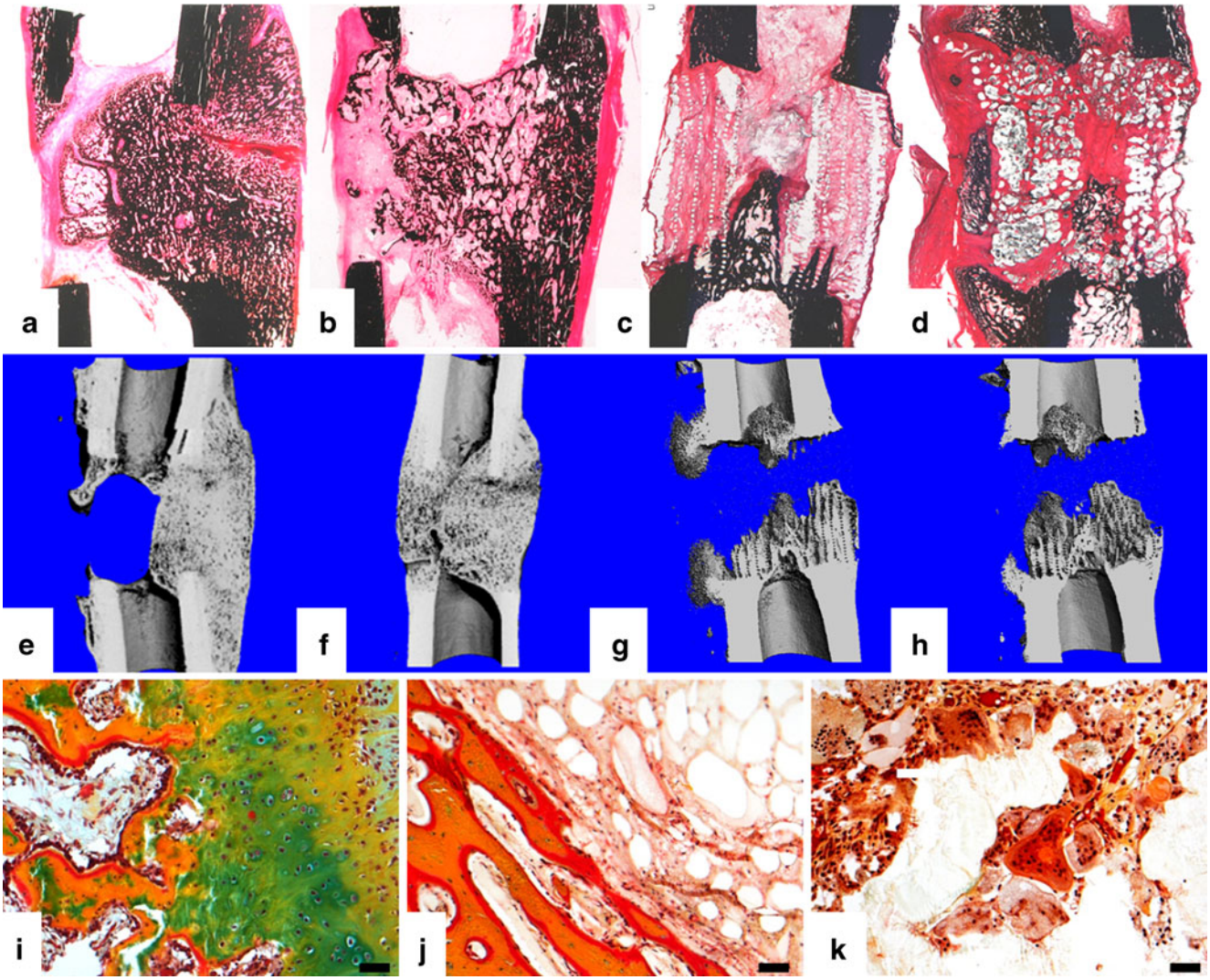

Fig. 4 Von Kossa/van Gieson staining on PMMA embedded specimens (**a**–**d**) showed extensive bone formation (*black*) and bridging in the autograft group (**b**, **f**), considerably less bone formation and non-union in the empty control (**a**, **e**) and the scaffold groups (mPCL-TCP: **c**, **g**; PDLLA-TCP-PCL: **d**, **h**). Histology results correlated well with 3-D microCT reconstructions of the defects (**e**–**h**). Movat's pentachrome staining (**i**–**k**) suggested endochondral bone formation in all groups (**i**, cartilage, *green*) with subsequent osteoid formation (**j**). In the autograft group, first signs of bone remodelling were evidenced by osteoclasts and giant cells within the defect area (**k**)

graded mechanical stiffness. Contact angle measurements have shown that such composite surfaces are more hydrophilic and that the degradation kinetics are accelerated three to four times compared to PCL alone. Biochemical advantages include improved cell seeding, and enhanced control and/or simplification of the incorporation and immobilisation of biological factors, such as bone morphogenetic proteins (BMP). So far, such composite scaffolds have been tested in a pig skull defect as well as in a spinal fusion model with promising outcomes [22]. In this study, the porosity of mPDLLA-TCP-PCL scaffolds had to be reduced significantly in order to achieve scaffolds with comparable mechanical properties to mPCL-TCP scaffolds.

To assess the effects of implanted bone grafts and tissue engineered constructions on segmental long bone defect regeneration, a number of large animal models have been established. In particular, mature sheep closely resemble human bone turnover and remodelling [23]. Moreover, sheep possess a body weight comparable to adult humans, and long bone dimensions enabling the use of human implants [24]. Osseous defects to study bone repair are postulated to be of dimensions precluding spontaneous healing [25]. These critical-sized defects are defined as the smallest size intraosseous wound in a particular bone and species of animal that will not heal spontaneously during the lifetime of the animal. Apart from size, a critical defect in long bones is influenced by factors such as species, anatomical location, associated periosteum and soft tissue, and biomechanical conditions in addition to age, metabolic and systemic influences and related comorbidities [26]. In

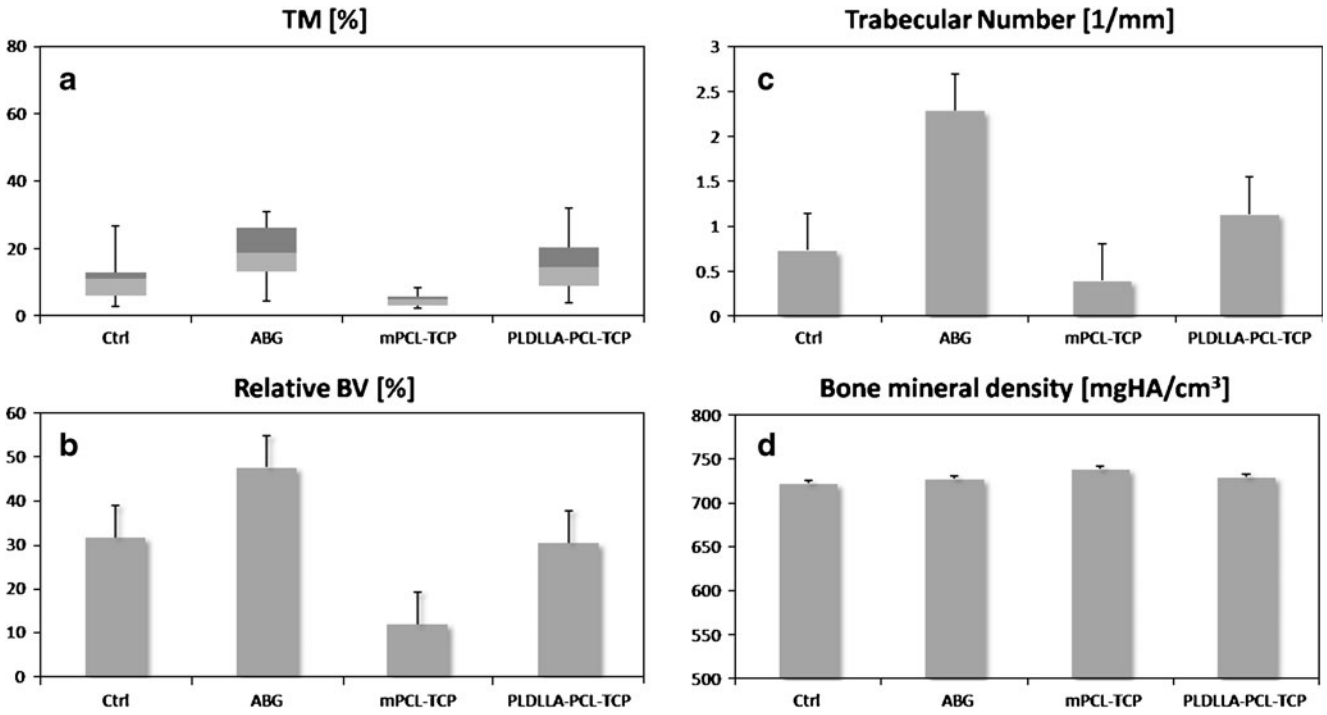

Fig. 5 Torsion testing data showed highest values for defect reconstructed with autograft (18.67%) when compared to untreated controls (11.19%) or defects treated with mPCL-TCP (4.96%) or PDLLA-TCP-PCL (14.41%) scaffolds (**a**). A similar trend was found for the relative bone volume formed within the defect (**b**) and the trabecular number (**c**) with highest values for autografts (47.64%; 2.28/mm^3) followed by defects treated with PDLLA-TCP-PCL (30.34%; 1.14/mm^3) scaffolds, empty controls (31.76%; 0.73/mm^3) and mPCL-TCP-treated defects (11.96%; 0.39/mm^3). No difference in bone mineral density was found (**d**). Mechanical testing data are presented as *box plots* and the microCT data as *bar graphs* with *error bars* representing standard deviations

our study a defect size of 2 cm was chosen since a previous literature search had shown that a 2-cm defect was the smallest critical-sized defect described in sheep tibiae [24]. Nevertheless, it was proven to be not of critical size within the settings selected for this study.

In humans, intramedullary nailing is a commonly chosen treatment modality for diaphyseal fractures and defects of the lower extremity. Since these central load carriers are less susceptible to tilting in the frontal plane, custom-made intramedullary nailing systems have been applied for fixation of large segmental bone defects in animal models [24]. In the context of tissue engineering, however, intramedullary stabilisation can impede the placement of a solid, one-piece load-bearing scaffold and necessitates two surgical approaches. Alternatively, external fixators have been widely used as they offer versatility and ease of application [10]. However, with external fixators, healing periods are reported to be significantly longer [27], External fixators represent a burden exceeding the physiological circumference of the animal limb and are prone to infection and pin loosening, especially in long-term studies. Therefore, defect fixation with plates or internal fixators offers considerable advantages. In this study, however, the 4.5-mm narrow LC-LCP might not have been strong enough as plate bending occurred in some animals. Due to the flexibility of the fixation device, callus formation (posterolaterally) was observed in the non-treated controls. It was concluded that the implant deformation resulted from critical loads (valgus stress) occurring during the act of the animal standing up from a lying position. However, while the implant was proven not to be strong enough in an immediately fully weight-bearing animal model, this should not be interpreted as having implications for the treatment of similar conditions in humans, since compliant patients can be advised to only partially weight bear and to avoid critical loads that might cause implant failure.

Both scaffold types under investigation did not perform as well as the gold standard treatment represented by the ABG. Both scaffolds showed good biocompatibility and sufficient mechanical strength. Combining a novel, biocompatible and biomechanically suitable scaffold such as mPCL-TCP or PDLLA-TCP-PCL with osteogenic cells (mesenchymal stem cells, osteoblasts) or a bone growth stimulating agent, e.g. recombinant human BMP 7 (rhBMP-7) [28–31], may enhance the treatment of large segmental bone defects without the need for vascularised autografts, non-vascularised autografts and/or allografts and could therefore represent a clinical alternative to bone autografts for the reconstruction of large tibial and femoral defects.

Acknowledgements The work was supported by Prof. Hutmacher's QUT start up grant, the Wesley Research foundation and the Australian Research Council (grant number 241402-0122.51).

Conflict of interest The authors declare that they have no conflict of interest.

References

1. Laurencin C, Khan Y, El-Amin SF (2006) Bone graft substitutes. Expert Rev Med Devices 3:49–57
2. Wildemann B, Kadow-Romacker A, Pruss A, Haas NP, Schmidmaier G (2007) Quantification of growth factors in allogenic bone grafts extracted with three different methods. Cell Tissue Bank 8:107–114
3. Pecina M, Vukicevic S (2007) Biological aspects of bone, cartilage and tendon regeneration. Int Orthop 31:719–720
4. Perry CR (1999) Bone repair techniques, bone graft, and bone graft substitutes. Clin Orthop Relat Res 360:71–86
5. DeCoster TA, Gehlert RJ, Mikola EA, Pirela-Cruz MA (2004) Management of posttraumatic segmental bone defects. J Am Acad Orthop Surg 12:28–38
6. Clements JR, Carpenter BB, Pourciau JK (2008) Treating segmental bone defects: a new technique. J Foot Ankle Surg 47:350–356
7. Theos C, Koulouvaris P, Kottakis S, Demertzis N (2008) Reconstruction of tibia defects by ipsilateral vascularized fibula transposition. Arch Orthop Trauma Surg 128:179–184
8. Sheller MR, Crowther RS, Kinney JH, Yang J, Di Jorio S, Breunig T, Carney DH, Ryaby JT (2004) Repair of rabbit segmental defects with the thrombin peptide, TP508. J Orthop Res 22:1094–1099
9. den Boer FC, Wippermann BW, Blokhuis TJ, Patka P, Bakker FC, Haarman HJ (2003) Healing of segmental bone defects with granular porous hydroxyapatite augmented with recombinant human osteogenic protein-1 or autologous bone marrow. J Orthop Res 21:521–528
10. Liu G, Zhao L, Zhang W, Cui L, Liu W, Cao Y (2008) Repair of goat tibial defects with bone marrow stromal cells and beta-tricalcium phosphate. J Mater Sci Mater Med 19:2367–2376
11. Sanger C, Soto A, Mussa F, Sanzo M, Sardo L, Donati PA, Di Pietro G, Spacca B, Giordano F, Genitori L (2007) Maximizing results in craniofacial surgery with bioresorbable fixation devices. J Craniofac Surg 18:926–930
12. Hench LL, Polak JM (2002) Third-generation biomedical materials. Science 295:1014–1017
13. Hollister SJ (2005) Porous scaffold design for tissue engineering. Nat Mater 4:518–524
14. Schumann D, Ekaputra AK, Lam CX, Hutmacher DW (2007) Biomaterials/scaffolds. Design of bioactive, multiphasic PCL/collagen type I and type II-PCL-TCP/collagen composite scaffolds for functional tissue engineering of osteochondral repair tissue by using electrospinning and FDM techniques. Methods Mol Med 140:101–124
15. Hutmacher DW, Schantz JT, Lam CX, Tan KC, Lim TC (2007) State of the art and future directions of scaffold-based bone engineering from a biomaterials perspective. J Tissue Eng Regen Med 1:245–260
16. Lam CX, Hutmacher DW, Schantz JT, Woodruff MA, Teoh SH (2009) Evaluation of polycaprolactone scaffold degradation for 6 months in vitro and in vivo. J Biomed Mater Res A 90:906–919
17. Movat HZ (1955) Demonstration of all connective tissue elements in a single section; pentachrome stains. AMA Arch Pathol 60:289–295
18. Hutmacher DW, Cool S (2007) Concepts of scaffold-based tissue engineering–the rationale to use solid free-form fabrication techniques. J Cell Mol Med 11:654–669
19. Leiggener CS, Curtis R, Müller AA, Pfluger D, Gogolewski S, Rahn BA (2006) Influence of copolymer composition of polylactide implants on cranial bone regeneration. Biomaterials 27:202–207
20. Helling HJ, Prokop A, Schmid HU, Nagel M, Lilienthal J, Rehm KE (2006) Biodegradable implants versus standard metal fixation for displaced radial head fractures. A prospective, randomized, multicenter study. J Shoulder Elbow Surg 15:479–485
21. Agarwal S, Gupta A, Grevious M, Reid RR (2009) Use of resorbable implants for mandibular fixation: a systematic review. J Craniofac Surg 20:331–339
22. Abbah SA, Lam CX, Hutmacher DW, Goh JC, Wong HK (2009) Biological performance of a polycaprolactone-based scaffold used as fusion cage device in a large animal model of spinal reconstructive surgery. Biomaterials 30:5086–5093
23. Pearce AI, Richards RG, Milz S, Schneider E, Pearce SG (2007) Animal models for implant biomaterial research in bone: a review. Eur Cell Mater 13:1–10
24. Reichert JC, Saifzadeh S, Wullschleger ME, Epari DR, Schütz MA, Duda GN, Schell H, van Griensven M, Redl H, Hutmacher DW (2009) The challenge of establishing preclinical models for segmental bone defect research. Biomaterials 30:2149–2163
25. Einhorn TA (1999) Clinically applied models of bone regeneration in tissue engineering research. Clin Orthop Relat Res 367:S59–S67
26. Lindsey RW, Gugala Z, Milne E, Sun M, Gannon FH, Latta LL (2006) The efficacy of cylindrical titanium mesh cage for the reconstruction of a critical-size canine segmental femoral diaphyseal defect. J Orthop Res 24:1438–1453
27. Konrad G, Südkamp N (2007) Extra-articular proximal tibial fracture (in German). Chirurg 78:161–171
28. White AP, Vaccaro AR, Hall JA, Whang PG, Friel BC, McKee MD (2007) Clinical applications of BMP-7/OP-1 in fractures, nonunions and spinal fusion. Int Orthop 31:735–741
29. Bishop GB, Einhorn TA (2007) Current and future clinical applications of bone morphogenetic proteins in orthopaedic trauma surgery. Int Orthop 31:721–727
30. Faria ML, Lu Y, Heaney K, Uthamanthil RK, Muir P, Markel MD (2007) Recombinant human bone morphogenetic protein-2 in absorbable collagen sponge enhances bone healing of tibial osteotomies in dogs. Vet Surg 36:122–131
31. Pluhar GE, Turner AS, Pierce AR, Toth CA, Wheeler DL (2006) A comparison of two biomaterial carriers for osteogenic protein-1 (BMP-7) in an ovine critical defect model. J Bone Joint Surg Br 88:960–966